Weakly noisy chaotic scattering

Juan D. Bernal,[*] Jesús M. Seoane, and Miguel A. F. Sanjuán

Nonlinear Dynamics, Chaos and Complex Systems Group, Departamento de Física, Universidad Rey Juan Carlos, Tulipán s/n,
28933 Móstoles, Madrid, Spain

The effect of a weak source of noise on the chaotic scattering is relevant to situations of physical interest. We investigate how a weak source of additive uncorrelated Gaussian noise affects both the dynamics and the topology of a paradigmatic chaotic scattering problem as the one taking place in the open nonhyperbolic regime of the Hénon-Heiles Hamiltonian system. We have found long transients for the time escape distributions for critical values of the noise intensity for which the particles escape slower as compared with the noiseless case. An analysis of the survival probability of the scattering function versus the Gaussian noise intensity shows a smooth curve with one local maximum and with one local minimum which are related to those long transients and with the basin structure in phase space. On the other hand, the computation of the exit basins in phase space shows a quadratic curve for which the basin boundaries lose their fractal-like structure as noise turned on.

I. INTRODUCTION

Chaotic scattering in open Hamiltonian systems has been an area of study in nonlinear dynamics, with applications in numerous fields in physics (see Refs. [1,2]). The context of this problem takes place in the motion of a particle in a potential well (Refs. [3–6]). In general, there exists a region where interactions between scattering particles and the potential occur, whereas outside this region the potential is negligible so that the particle motions are essentially free. This region is typically called the *scattering region*. For many potential functions of physical interest, evolution equations are nonlinear resulting in chaotic dynamics in the scattering region. Since the system is open, this region possesses exits for which the particles may enter or escape. Due to the chaotic dynamics in the scattering region, slightly close initial conditions have trajectories which spend different times inside the region and may escape taking different directions. Quite often, particles starting in the scattering region bounce back and forth for a finite time before escaping. In this sense chaotic scattering could be presented as a physical manifestation of transient chaos ([7,8]).

Most previous works have been devoted to purely conservative systems ([4–6]), and, more recently, the effects of weak dissipation on chaotic scattering have been addressed ([9–11]). Despite a large body of existing literature on chaotic scattering, there have been few works on the effect of noise on certain characteristics of scattering dynamics ([12–14]). For instance, in Ref. [12], the escapes from a driven potential well system and the estimation of the average escape time in a noisy environment were addressed. The latest works on the effects of external noise in open Hamiltonian systems have shown that, for a certain range of noise intensities ($\sim 10^{-3}$), the decay law of the scattered particles is exponential and the phase space is completely blurred, exhibiting a ful destruction of the boundary fractality and the KAM islands structure [14–16]. Finally, a detailed investigation [17] of the Hénon map shows

that noise can also play a constructive role in chaotic scattering, enhancing the trapping of trajectories.

Within the present work, we will study a dynamical system model which describes the behavior of scattering particles in a two-dimensional potential, the Hénon-Heiles system, under the effect of an external source of weak additive uncorrelated Gaussian noise. We will focus our numerical computations on the regime of mechanical energies where the Hénon-Heiles system exhibits an open nonhyperbolic dynamic. One of the most accurate algorithms for stochastic processes resolution is the second-order Heun algorithm [18] as was shown in Ref. [14]. The fact that a certain source of weak noise is unavoidable in any physical system has motivated us to investigate more thoroughly this constructive role in a quantitative manner. This allows us to generalize the previous results from maps [17] to flows, studying the effects of noise in phase space and proposing a conjecture to explain the theoretical basis of the aforesaid noise constructive effects. The main findings of this work concern the effects of weak noise in both the decay law of the particles in the scattering region and the exit basins associated to phase space. The presence of weak noise [17] implies the existence of long transients for the particles in the scattering region. On the other hand, the analysis of the characteristic time versus the noise intensity shows a curve with one local maximum and one local minimum which are related to the long transients in the scattering region and with the persistence of KAM islands in noisy environments. In addition, the computation of the exit basins shows a quadratic curve between the noise intensity and the energy for which the KAM islands are destroyed. These last behaviors are properly explained by using some heuristic arguments.

This paper is organized as follows. In Sec. II we describe our prototype model, the Hénon-Heiles system. The effects of a weak source of additive uncorrelated Gaussian noise on the decay law of the particles in the scattering region are examined in Sec. III. In Sec. IV we study the influence of a weak noise on the basin structure of the exit basins associated with phase space. Heuristic arguments of the previous results are shown in Sec. V. A discussion and the main conclusions of this manuscript are presented in Sec. VI.
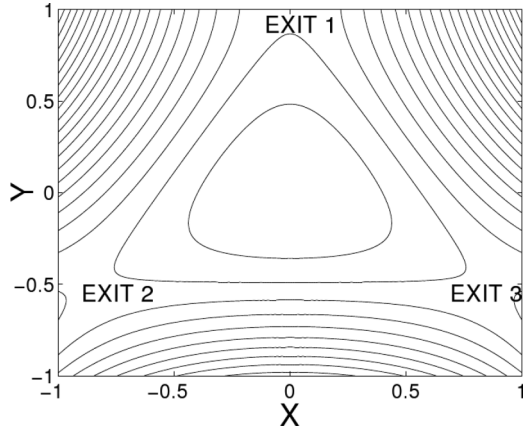
*jdbernalf@gmail.com

FIG. 1. Isopotential curves for the Hénon-Heiles potential. They are closed for energies below $E_e = 1/6$, but it shows three different exits for energy values above $E_e = 1/6$.

II. MODEL DESCRIPTION

In this section we study the dynamics of chaotic scattering in a noisy environment. In order to show the dynamics of this kind of systems we use the Hénon-Heiles Hamiltonian system, which is described by

$$H = \tfrac{1}{2}(\dot{x}^2 + \dot{y}^2) + \tfrac{1}{2}(x^2 + y^2) + x^2 y - \tfrac{1}{3} y^3. \qquad (1)$$

This conservative two-dimensional model was developed by astronomers Michel Hénon and Carl Heiles in 1964 to describe the dynamical behavior of axisymmetrical galaxies [3]. The isopotential curves of the Hénon-Heiles system can be seen in Fig. 1. There are two different sorts of motions in the Hénon-Heiles system, which correspond to bounded ($E_0 \in [0, 1/6]$) and unbounded orbits (for $E_0 > 1/6$). Therefore, depending on the value of the energy, the orbit is trapped in the scattering region or escapes from it up to infinity. In fact, there are three different regimes of motion depending on the initial value of the energy: $E_0 \in [0, 1/6]$, $E_0 \in (1/6, \simeq 0.22)$, and $E_0 \in [\simeq 0.22, \infty]$ [19]. Within the first energy range, the regime of motion is closed and nonhyperbolic, so all the orbits are trapped, and there is no exit by which any particle may escape. There is a wide variety of possible motions in this energy range, from periodic and quasiperiodic orbits to chaotic trajectories. However, in the range of $E_0 \in (1/6, \simeq 0.22)$ the regime is open and nonhyperbolic, the energy is high enough to allow escapes from the scattering region, and the existence of KAM tori coexists with chaotic saddles, which typically results in an algebraic decay in the survival probability of a particle in the scattering region. We state that KAM islands have a certain stickiness [20]. On the contrary, if $E_0 \in [0.22, \infty]$, the regime is open and hyperbolic, all the periodic orbits are unstable, and therefore there is no KAM island in phase space.

Due to the triangular symmetry of the system, the exits are separated by an angle of $2\pi/3$ radians. For the sake of clarity we call exit 1 the upper exit ($y \to +\infty$), exit 2 the left one ($y \to -\infty, x \to -\infty$), and exit 3 the right exit ($y \to -\infty, x \to +\infty$).

The aim of the present work is concentrated on the dynamical behavior of the particles in the open nonhyperbolic regime, $E_0 \in (1/6, 0.22)$, under the effect of a weak source of additive uncorrelated Gaussian noise. When we introduce
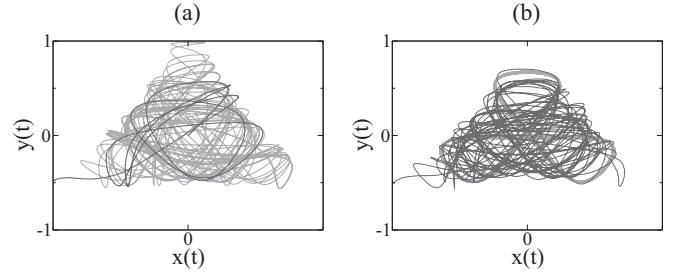

FIG. 2. Comparison between different kind of orbits with additive uncorrelated Gaussian noise of weak intensity $\xi = 10^{-5}$, in black, and noiseless, in gray. Orbits corresponding to particles shot from the initial condition $(x, y) = (0, 0)$ with $E_0 = 0.19$. The shooting angle are (a) $\varphi = 3\pi/10$; (b) $\varphi = \pi$.

a Gaussian noise as previously defined in the Hénon-Heiles system, the equations of motion are given by [14]

$$\begin{aligned} \ddot{x} &= -x - 2xy + \sqrt{2\xi}\, dW_x, \\ \ddot{y} &= -y - x^2 + y^2 + \sqrt{2\xi}\, dW_y, \end{aligned} \qquad (2)$$

where ξ is the intensity of the Gaussian noise and $dW_{x,y}$ are the Wiener stochastic processes. The Wiener process W_t has independent increments with $W_t - W_s \sim N(0, t - s)$ (for $0 \leqslant s < t$), where $N(\mu, \sigma^2)$ denotes the normal distribution with mean μ and variance σ^2. Equivalently, we may state that $W_t - W_s \sim \sqrt{(t - s)} N(0, 1)$ with $W_0 = W(0) = 0$. Therefore, according to Eq. (2), $\sqrt{2\xi}\, dW \sim \sqrt{2\xi(t - s)} N(0, 1)$, which denotes a normal distribution with mean $\mu = 0$ and variance $\sigma^2 = \sqrt{2\xi(t - s)}$.

In order to get a qualitative insight about the effect of a very weak Gaussian noise as previously, for instance, $\xi = 10^{-5}$, we represent in Figs. 2(a)–(b) different particle orbits under the effect of noise, in black, and their noiseless equivalent, in gray. The effect of noise, even with a very low intensity ($\xi = 10^{-5}$), yields a significantly different result. Therefore, the initial conditions chosen for both panels (a) and (b) in the noiseless case result in trapped trajectories. However, the same initial conditions under the effect of a very low noise come from orbits that leave the scattering region after a finite time. According to Fig. 2(a), the particle described by the black trajectory leaves the scattering region through exit 2 a few time steps since the beginning of the iterations. Likewise, the particle in black also leaves the scattering region by exit 2, but after a long transient time, as shown in Fig. 2(b).

Since the noise intensity introduced in Eq. (2) via the Wiener process is very low $\xi \in [10^{-10}, 10^{-5}]$, it might be possible that the numerical noise blurs the real effect of this physical noise on the particle dynamics. Actually the aforesaid numerical noise is inherent to the computation of any trajectory since it arises at each iterative calculation. It is worth noting that we have studied both the convergence and the stability of the numerical scheme arranged by a second-order Heun algorithm [18] for the resolution of the stochastic processes shown in Eq. (2) as was previously used in Ref. [14]. We have undertaken a sensitivity analysis in order to choose the most suitable temporal discretization scheme h for each considered noise intensity, such that h ensures the convergence and the stability of the solution with a reasonable computational cost.
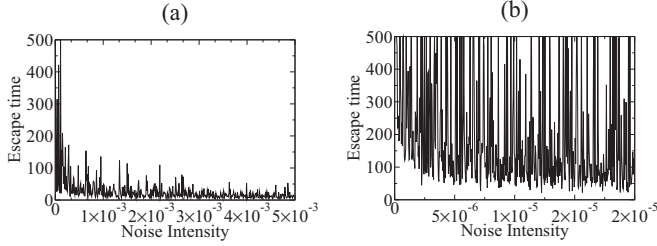
FIG. 3. Escape time of a single particle under the effect of a Gaussian noise. The initial conditions are $(x, y) = (0,0)$ and $\varphi = 0.0$ with $E_0 = 0.19$. The noise intensities are (a) $0.0 < \xi \leqslant 5 \times 10^{-3}$ and (b) $0.0 < \xi \leqslant 2 \times 10^{-5}$.

Moreover, the dynamics of the noisy Hénon-Heiles system is compared by using two different stochastic integratros: the second-order Heun algorithm and the Greenside and Helfand method (see Ref. [21]), which is more robust. According to the numerical computations, we can state that the results obtained by both algorithms are consistent and equivalent for the purposes of this paper.

III. EFFECTS OF A WEAK GAUSSIAN NOISE ON THE DECAY LAW

There are two important questions that need to be addressed regarding the effects of noise on the decay law: the average escape time of a set of initial conditions and the corresponding time delay statistics $P(t)$.

The *escape time* of an incident particle is defined as the time spent in the scattering region before escaping to infinity. For times above t_e, the particle travels to infinity after having crossed one of the three exit boundaries, which are extremely unstable orbits called *Lyapunov orbits* (see Ref. [22]). Lyapunov orbits exist for energies higher than $1/6$. It is quite obvious that the higher the energy, the shorter escape times, but in a nonhyerbolic regime there are always certain orbits that remain forever in the scattering region. The escape time of a single particle with an initial shooting angle $\varphi = 0.0$ under the effect of a Gaussian noise is shown in Fig. 3(a). We zoom in this last figure for very small values of the noise intensity in Fig. 3(b). We can observe that for high noise intensities ($\sim 10^{-3}$), the escape time approaches zero, which means that all the particles escape. However, for low values of the noise intensity ($\sim 10^{-5}$) the escape times are larger, meaning that the particles get trapped in the scattering region.

We have numerically studied the influence of the variation of the intensity of a weak Gaussian noise on the average escape time of a set of initial conditions. Looking for that purpose, we shoot 10 000 particles from the point D of the phase space, $D = (x_0, y_0, \dot{x}_0, \dot{y}_0) = (0,0,v\cos(\varphi), v\sin(\varphi))$, with an energy $E_0 = 0.19$, initial angle $\varphi \in [0, 2\pi]$ and initial velocity

$$v = \sqrt{2E_0 - x_0^2 - y_0^2 - 2x_0^2 y_0 + \frac{2}{3}y_0^2}.$$

We have simulated the effects of different noise intensities (200 variations from $\xi = 0.0$ to $\xi = 5.0 \times 10^{-5}$, with an incremental step of $\triangle\xi = 2.5 \times 10^{-7}$).

Contrary to what might be initially thought, when the noise intensity is very weak, up to $\sim 10^{-5}$, the averaged t_e grows as long as the noise increases, as can be observed in Fig. 4. This
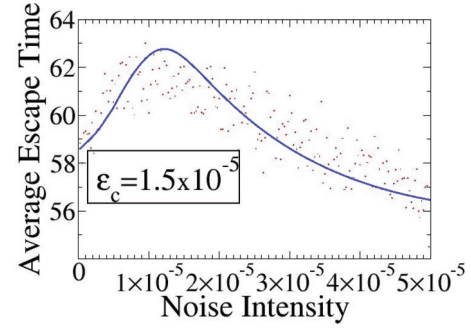

FIG. 4. (Color online) Average escape time of 10 000 particles with initial conditions $(x_0, y_0, \dot{x}_0, \dot{y}_0) = (0,0,v\cos(\varphi), v\sin(\varphi))$, with an energy, $E_0 = 0.19$, and shooting angle, $\varphi \in [0, 2\pi]$. There are 200 variations of the noise intensity, from $\xi = 0.0$ to $\xi = 5.0 \times 10^{-5}$, with an incremental step of $\triangle\xi = 2.5 \times 10^{-7}$. The blue (black) line is used to help the eye to get a better insight of the trend of the points.

trend is kept until the noise intensity overtakes a threshold value, 1.5×10^{-5}. For intensity values above 1.5×10^{-5}, the external perturbation is large enough to destabilize the system, destroying the KAM islands very fast and prompting that the decay law of the particles becomes exponential. Therefore it is seen that t_e decreases so quickly, as is well explained in Ref. [14].

Another fundamental aspect of chaotic scattering is the time delay statistics $P(t)$. We pick many b values at random in some interval of the domain. We then examine the resulting orbit for each value and determine the time t that its orbit spends in the scattering region. The fraction of orbits with *time delay* between t and $t + dt$ is $P(t)\,dt$. For open nonhyperbolic dynamics in the absence of noise with bounding KAM surfaces in the scattering region, one finds that for large t the time delay statistics, $P(t)$, decays algebraically as

$$P(t) \sim t^{-\alpha}. \tag{3}$$

Likewise, the particle decay law for noiseless open hyperbolic dynamics is

$$P(t) \sim e^{-t/\tau}, \tag{4}$$

where τ is a characteristic time for the scatterer.

The works undertaken by Seoane *et al.* [14,15] demonstrated that an external source of Gaussian noise relatively weak, $\xi \approx 1 \times 10^{-3}$, fully destroys the KAM island, driving the system to a hyperbolic regime and prompting that the decay law is exponential. Our current research has shown that the Hénon-Heiles systems does not have this behavior if the noise intensity is low enough. For noise intensities lower than $\xi = 1.5 \times 10^{-5}$, the decay law of the time delay statistics is algebraic according to Eq. (3) as shown in Fig. 5(a). Nonetheless, for noises larger than the aforesaid threshold value, the algebraic decay is not valid anymore, and we have to resort to exponential decay as exhibits in Fig. 5(b).

It is worth noting that, in the most general sense, we define scattering as the problem of obtaining the relationship between an "input" variable taken from outside the scattering region and an "output" variable, which characterizes the final state of the system after interacting with the scattering region (see Ref. [2]). However, the fact of starting the numerical experiments inside the scattering region is a convention frequently
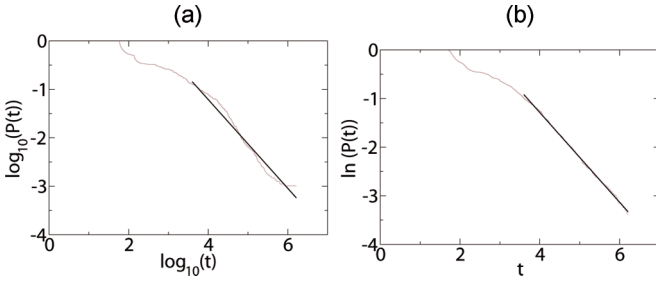
FIG. 5. (Color online) For energy $E_0 = 0.19$. (a) Weak noise intensity $\xi = 1 \times 10^{-5}$; the resulting graphic is $\log_{10}[P(t)]$ vs $\log_{10}(t)$ since the decay law results algebraic according to Eq. (3). (b) For higher intensities than $\xi = 1 \times 10^{-5}$, in this particular case a weak noise of intensity 5×10^{-5}, the algebraic decay is not valid anymore, and we have to resort to an exponential decay, $\ln[P(t)] \sim t$, as explained in Ref. [15].

used in the scientific literature (see, for example, Refs. [14–16] and [19]). The reason behind this is to take advantage of the well-known topological structure of the escape basins resulting from the Poincaré surface of section $(\dot{y}, y)$ for $x(0) = 0$. Therefore it is implicitly assumed that the initial conditions chosen for the computations may correspond to trajectories that come from outside the scattering region, and, after bouncing back and forth for a certain time in the scattering region, they pass through $x = 0$ with a certain velocity $(\dot{x}, \dot{y})$. This is the precise instant when the simulations start, and the initial conditions are set as $(x = 0, y, \dot{x}, \dot{y})$. This aspect is quite relevant since the scaling exponent of the time delay functions change by one depending on whether the initial conditions are taken inside rather than outside the scattering region (see Ref. [23]).

Focusing our attention within the algebraic range, we can study another interesting feature from the behavior of the decay law while the noise intensity increases: the evolution of the parameter α from Eq. (3). Parameter α is directly proportional to the average speed by which the particles leave the scattering region because α is the exponent of t in Eq. (3). The higher the α, the faster decays $P(t)$, and, therefore, the quicker the particles exit from the scattering region. From $\xi = 0$ to a certain value of the noise intensity, $\sim 10^{-7}$, α increases while the noise intensity also grows, as can be seen in Fig. 6. However, from values above $\sim 10^{-7}$ to a threshold value, $\sim 1 \times 10^{-5}$, the parameter α abruptly decreases, meaning that the particles escape from the scatterer much slower than before. Once the noise exceeds this limit, α starts to increase rapidly according to an exponential decay law, as has been clearly explained in Refs. [15] and [16]. It is really worth noting that 1.5×10^{-5} is the same threshold value where the curve $\overline{t_e} = \overline{t_e}(\xi)$ exhibits a global maximum (Fig. 4). In the same way, it is the one where the curve $\alpha = \alpha(\xi)$ shows a global minimum (Fig. 6), and the same value where the algebraic decay law of $P(t)$ is not valid anymore. A further explanation of the evolution of α with the noise intensity is described in Sec. IV and Fig. 9. It is worth noting that the relation between the scaling factor α and the noise intensity is dependent on the range of noise intensities. The parameter α follows a linear trend with respect to the noise intensity for higher noises than the ones considered in the present work, from $\xi \sim 1 \times 10^{-4}$ on, as was shown in Ref. [14].
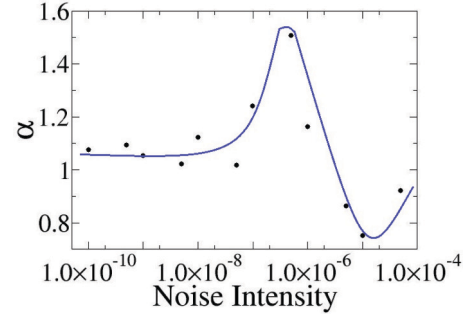

FIG. 6. (Color online) The value of the parameter α versus a set of noise intensities, $\xi = \{0, 1 \times 10^{-10}, 5 \times 10^{-10}, 1 \times 10^{-9}, 5 \times 10^{-9}, \ldots, 1 \times 10^{-5}, 5 \times 10^{-5}\}$ for energy $E_0 = 0.19$ is shown. There is a local minimum around $\sim 1 \times 10^{-5}$ which fits to the local maximum as we saw in Fig. 4. Therefore, there is a point, $\sim 1 \times 10^{-5}$, where the noise intensity is just the one that maximizes $\overline{t_e}$. The reason behind the maximum about $\sim 1 \times 10^{-7}$ is explained at Sec. IV. The blue (black) line is used to help the eye to get a better insight of the trend of the points. The relation between the scaling factor α and the noise intensity is dependent on the range of noise intensities. Actually α follows a linear evolution with respect to the noise intensity for higher noises than the ones considered in the present work, from $\xi \sim 1 \times 10^{-4}$ on, as was demonstrated in Ref. [14].

IV. EFFECTS OF A WEAK GAUSSIAN NOISE ON THE BASIN TOPOLOGY

One topic of interest with regard to the effect of noise on open Hamiltonian systems which has been broadly studied [24,25] is the evolution of the exit basins topology of the Hénon-Heiles system while the noise is increased within a range of relatively weak intensities, $\xi \sim 1 \times 10^{-3}$. However, we have especially focused our attention on a range of weaker noises, where the system exhibits an algebraic decay law, as seen in Sec. III. The analyzed range covers from the noiseless case to the value where the KAM islands are fully destroyed and the fractal boundaries are significantly faded. We have then cross-checked that this value is the same as the one found in Sec. III.

We carry out different simulations in order to represent the Poincaré surface of section $(\dot{y}, y)$ for $t = 0$ and $x(0) = 0$, for each noise intensity considered. We have run different simulations to plot the exit basins of the Hénon-Heiles system for a wide range of noises, as shown in Fig. 7.

According to Fig. 7(a)–(c), for noise intensities lower than $\xi = 1.5 \times 10^{-5}$, the boundaries of each basin conserve the fractal-like structure. Nonetheless we can see how the KAM islands start to disappear for $\xi = 1 \times 10^{-7}$. The gradual destruction of the KAM islands is the responsible for the maximum shown in Fig. 6. As was pointed out in Refs. [26] and [27], the topological structures are conserved for weak perturbations. For noise intensity values above $\xi = 1.5 \times 10^{-5}$, the once rich fractal structure completely disappears and becomes shaded off, as shown in Fig. 7(d). When basin boundaries are fully blurred, we cannot distinguish at all which initial condition will escape by a certain exit, because they are mixed up in the phase space. Therefore, we can state that the noise intensity significantly increases the uncertainty of the system in these conditions.
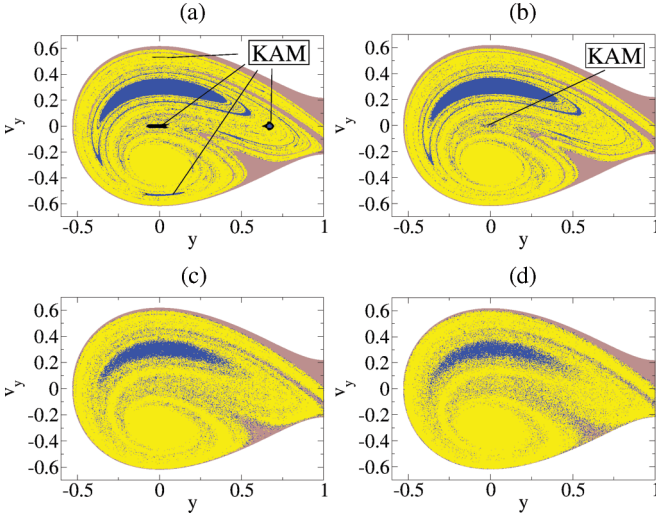
FIG. 7. (Color online) Set of figures where the exit basins of the Hénon-Heiles system for different noise intensities and $E_0 = 0.19$ are plotted. The sets of brown (gray), blue (dark gray), and yellow (light gray) dots denote initial conditions resulting in trajectories that escape through exits 1, 2, and 3 (see Fig. 1), respectively, and the black regions denote the KAM islands. (a) Weak noise, $\xi = 1 \times 10^{-10}$; (b) $\xi = 1 \times 10^{-7}$; (c) $\xi = 1.5 \times 10^{-5}$ is the threshold value according to Figs. 4 and 6 for which the fractal-like structure is hardly conserved; (d) $\xi = 4 \times 10^{-5}$. For (a–b), each basin boundary is fractal and not blurred. Indeed, they conserve their rich structure (although we can see as the KAM islands start to disappear for $\xi = 1 \times 10^{-7}$). The gradual destruction of the KAM islands is responsible for the maximum shown in Fig. 6. As was pointed out in Refs. [26] and [27], the topological structures are conserved for weak perturbations. Nonetheless, for noise intensities higher than $\xi = 1.5 \times 10^{-5}$, the once rich fractal structure completely disappears and becomes shaded off, as shown in (d).

Figure 8 represents the noise intensity where the exit basin boundaries are just blurred versus the energy of the Hénon-Heiles system. If we proceed with a nonlinear fitting of the curve, we can see that it matches with a second-order polynomial equation, such that: $\xi^* = a_0 + a_1 E_0 + a_2 E_0^2$ ($R = 0.999405$), with $a_0 = 6.67853 \times 10^{-4}$, $a_1 = -8.13772 \times 10^{-3}$, and $a_2 = 2.47492 \times 10^{-2}$. The reason for this is due to the fact that the threshold value of the noise intensity is correlated to the typical scale l_c of the fine structure of the
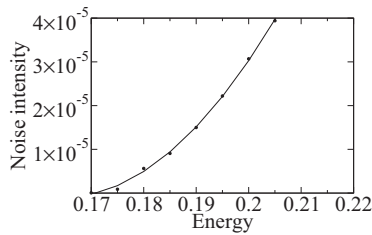

FIG. 8. This figure represents the noise intensity where the exit basin boundaries are just blurred vs the initial energy of the Hénon-Heiles system. The resulting curve matches with a second-order polynomial equation: $\xi^* = a_0 + a_1 E_0 + a_2 E_0^2$ ($R = 0.999405$), with $a_0 = 6.67853 \times 10^{-4}$, $a_1 = -8.13772 \times 10^{-3}$, and $a_2 = 2.47492 \times 10^{-2}$.
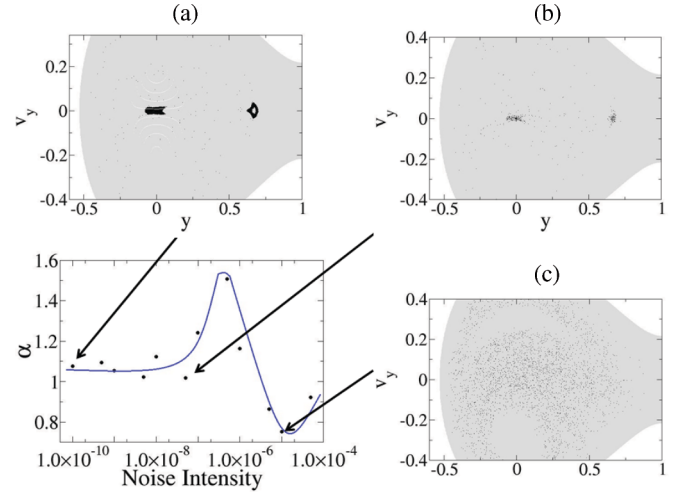

FIG. 9. (Color online) The group of panels (a–c) represents the evolution of the KAM islands in the phase space $(\dot{y}, y)$ as the noise increases for $E_0 = 0.19$. Gray regions denote initial conditions resulting in trajectories that escape through any of the three exits. Black dots are the particles remaining in the scattering region after times higher than t_{max}, as are the KAM islands. The aforesaid panels are related to their correspondent noise intensities by Fig. 6 in order to link them with the scaling factor α. (a) Weak noise, $\xi = 1.0 \times 10^{-10}$, KAM tori still keep their topological structures. (b) $\xi = 8.0 \times 10^{-8}$, the KAM islands start to be blurred. While the noise increase up to the local maximum of Fig. 6, the number of trapped particles decays abruptly. From this maximum on, the number of remaining particles, black dots, starts to raise again, spreading throughout the whole phase space. (c) $\xi = 1.5 \times 10^{-5}$ is the threshold value where there is a maximum number of trapped particles, uniformly spread along the whole phase space. For noises higher than $\xi = 1.5 \times 10^{-5}$, the number of trapped particles decays.

KAM tori [15] in a quadratic manner and, as we see in Sec. V, l_c is directly related to the value of $\overline{t_e}$.

An external weak noise can modify the stability of the KAM islands such that it breaks their topological structures. We have studied how an external source of weak noise can modify the stability of the KAM islands and its relation to the threshold value obtained in the previous sections ($\xi = 1.5 \times 10^{-5}$).

We can see the evolution of the KAM island topology with the noise increasing in the set of figures shown in Fig. 9. When the noise is really weak, $\xi \in [1 \times 10^{-10}, 8 \times 10^{-8}]$, the morphology of the KAM sets is similar to the noiseless case. However, once the noise intensity exceeds the upper limit of the aforementioned range, $\sim 8 \times 10^{-8}$, the KAM islands start to be blurred, and the number of particles which remains in the scattering region after t_{max} decreases abruptly. Nonetheless, if the noise intensity keeps growing, when it reaches a certain value close to $\xi \sim 5 \times 10^{-7}$, the number of trapped particles starts to rise and to be spread along the whole phase space. This behavior is conserved until $\xi \sim 1.5 \times 10^{-5}$, where the number of trapped particles is maximum and they are fully spread throughout the phase space. Taking into consideration that at $\xi \sim 5 \times 10^{-7}$ the curve $\alpha = \alpha(\xi)$ shows a global maximum and, for noise intensity values above that limit, $\alpha = \alpha(\xi)$ decays, we can state that the stickiness formerly given by the KAM sets now loses intensity but gains extension. Therefore,

the more particles remain in the scattering region, the higher is t_e because it is likely that these bounded particles drive the average $\overline{t_e}$ up to higher values. This trend is kept until $\alpha = \alpha(\xi)$ reaches a global minimum at $\xi \sim 1.5 \times 10^{-5}$.

V. QUALITATIVE ANALYSIS OF THE EXTERNAL GAUSSIAN NOISE EFFECTS

We have developed a qualitative analysis to explain the reason behind the increase of the average escape time $\overline{t_e}$ when the noise also increases for a certain range of intensities until the threshold value (see Fig. 4).

We conjecture that every single point of any trajectory of a noisy Hénon-Heiles system can be matched with a single point of one of the different noiseless orbits of the Hénon-Heiles system by a one-to-one function. Because of the existence of noise, the mechanical energy is not conserved and the points of a noisy trajectory belong to different noiseless orbits with different energy values. Therefore, we can consider that any solution of a noisy system travels throughout various noiseless trajectories of the Hénon-Heiles system.

For the sake of clarity, we call hereinafter *KAM* or *trapped trajectories* such invariant sets of a noiseless system that, starting from a point of a KAM island, are trapped in the scattering region forever. In the same way, we call a *KAM region* of a noiseless system any subdomain of the phase space that contains *trapped orbits* in a certain time t.

Following our conjecture we can explain the fact that regardless the intensity of the external perturbation, there are no bounded trajectories for $t \to \infty$ if $\xi > 0$ [29]. The trajectory of any initial condition that in the noiseless case belongs to a KAM island in the absence of noise would jump randomly for a certain period of time among trapped noiseless trajectories. However, the noisy trajectory cannot jump among the KAM orbits for $t \to \infty$ because there is always a nonzero probability of jumping from the noiseless KAM region to outside, diverging to infinity.

Now we focus our attention in the range of noise intensities where the average escape time $\overline{t_e}$ increases insofar the external weak noise also increases until getting the maximum shows in Fig. 4. According to the aforesaid conjecture, there are initial conditions that in the noiseless case are outside a KAM island, but, due to the effect of noise, they can jump into a region where there are noiseless trapped trajectories, and then they can randomly walk through them during a certain period of time. In that case, it is likely that the particle has a higher escape time t_e than its noiseless equivalent because its jumps in that region normally represent a delay. Since there are many more particles outside the KAM islands than inside them, this effect exceeds the hypothetical reduction of t_e due to the effect of jumps from inside to outside. Likewise, as the noise intensity slightly increases, there are more particles outside the KAM islands that are allowed to jump into them. That is why the average escape time $\overline{t_e}$ grows when the external weak noise increases.

When the noise is higher than a threshold value (see Fig. 4), the jump intensity is very high and most particles cannot reach a KAM region because the distance traveled due to the noise is very long. For the same reason, the initial conditions of the noiseless trapped orbits jump outside faster than before. The optimum noise intensity should be the one that maximizes the escape time t_e. That is, high enough to promote that the maximum number of particles coming from outside can reach KAM trajectories, but at the same time, low enough to avoid quick and generalized jumps outside the KAM island. The threshold value of the noise intensity is directly related to the typical scale l_c of the structure of the KAM tori [15].

According to Fig. 6, any noise increase from ($\xi = 0$) to ($\xi \sim 5 \times 10^{-7}$) involves a faster escape of the particles from the scattering region. We consider that the jumps of the noisy orbits throughout the KAM region are very short and cannot compensate for the effect in the average escape time $\overline{t_e}$ of the particles that leave the KAM region at the first iterations due to the noise. The jumps are very short because trapped trajectories diverge faster in each iteration than the distance covered by the jump between these orbits.

After this qualitative conjecture, we now propose a theoretical framework to explain the reason why the increase of the noise intensity up to a certain threshold value yields higher average escape times.

We consider that the external Gaussian noise affects only the kinetic energy of the particles, but it does not influence at all the potential energy of the Hénon-Heiles system because its intensity is very weak.

Therefore, the equations of motion of the Hénon-Heiles system can be written as

$$\ddot{x} = \frac{\partial V}{\partial x} + \xi_x(t), \quad \ddot{y} = \frac{\partial V}{\partial y} + \xi_y(t). \quad (5)$$

Getting the total derivate of the mechanical energy, $E = T + V$, taking into consideration that $V = V(x,y)$, $T = T(\dot{x}, \dot{y})$ and using Eq. (5), $\frac{\partial V}{\partial x} = \ddot{x} - \xi_x(t)$ and $\frac{\partial V}{\partial y} = \ddot{y} - \xi_y(t)$, then we obtain

$$\frac{dE}{dt} = \dot{x}[2\ddot{x} - \xi_x(t)] + \dot{y}[2\ddot{y} - \xi_y(t)]$$

$$= 2\frac{dT}{dt} - [\dot{x}\xi_x(t) + \dot{y}\xi_y(t)],$$

$$\frac{dV}{dt} = \frac{dT}{dt} - [\dot{x}\xi_x(t) + \dot{y}\xi_y(t)]. \quad (6)$$

Integrating between the initial time $t = 0$ and the escape time $t = t_e$:

$$V_e - V_0 = T_e - T_0 - \int_0^{t_e}[\dot{x}\xi_x(t) + \dot{y}\xi_y(t)]\,dt. \quad (7)$$

We initially shot the particle from $(x,y) = (0,0)$, then $V_0 = 0$ and $T_0 = E_0$. Moreover, because of we stated that external Gaussian noise does not affect the potential energy of the Hénon-Heiles system and that outside the scattering region the potential is negligible (see Sec. I), $V_e = 0$. Otherwise, the initial energy E_0 would not be conserved from $t = 0$ to the escape time $t = t_e$ in the noiseless Hénon-Heiles after substituting $\xi_x(t)$ and $\xi_y(t)$ by zero in Eq. (7).

Therefore,

$$T_e - T_0 = \int_0^{t_e}[\dot{x}\xi_x(t) + \dot{y}\xi_y(t)]\,dt. \quad (8)$$

The above integral has dimensions of energy, so we can say that this is a random energetic contribution of the external
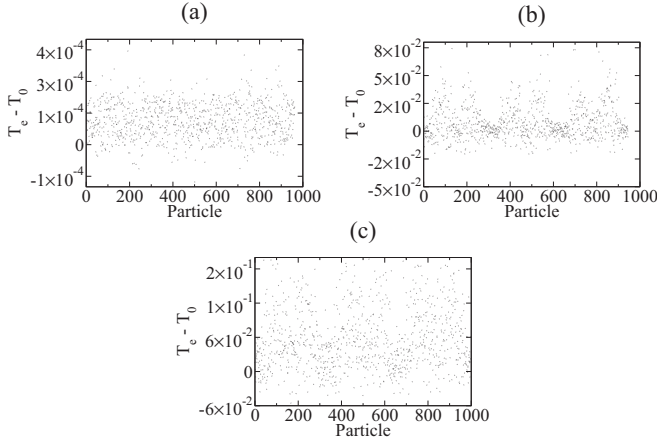
FIG. 10. This set of figures shows the difference between the kinetic energy of a particle when its trajectory leaves forever the scattering region and its initial kinetic energy $T_e - T_0$. All the particles are launched with an initial energy of $E_0 = 0.19$, for three noise intensities: (a) $\xi = 1 \times 10^{-10}$; (b) $\xi = 1.5 \times 10^{-5}$; (c) $\xi = 5 \times 10^{-4}$. The data dispersion increases as the noise intensity grows. When the noise intensity increases, the variance σ^2 of $T_e - T_0$ increases accordingly.

noise to the total mechanical energy. Furthermore, if there is no external noise, then $T_e = T_0$. The reason why T_e differs from T_0 is the velocity fluctuation due to the existence of noise, $\xi_x(t)$ and $\xi_y(t)$. Therefore, we can state that $T_e - T_0 \sim N(0, \sigma^2)$, where σ^2 is the variance of the normal distribution $T_e - T_0$ due to the effect of noise. The higher the noise intensity, the more dispersed are the data of the distribution $T_e - T_0$ (see Fig. 10). Insofar the noise intensity increases, the variance σ^2 of $T_e - T_0$ increases accordingly.
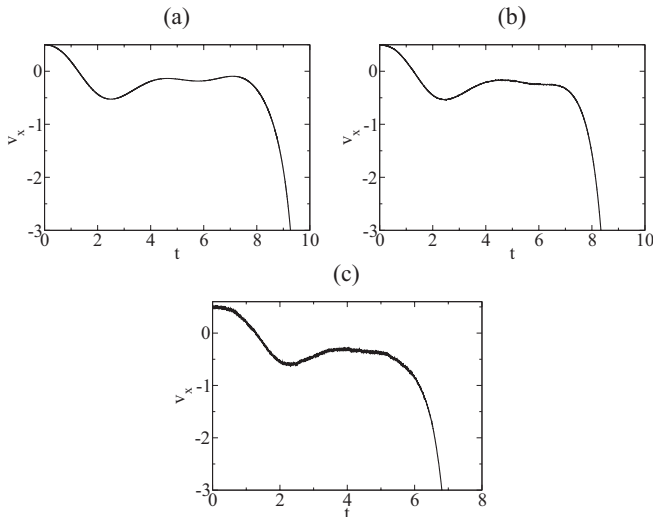

FIG. 11. This set of figures represents the x component of the velocity versus time t of a particle shot from (x, y) with initial energy $E_0 = 0.19$ and initial angle $\varphi = \pi/5$. (a) $\xi = 1 \times 10^{-10}$; (b) $\xi = 1.5 \times 10^{-5}$; (c) $\xi = 5 \times 10^{-4}$. For low noise intensities (cases a–b), the particle velocity is not very influenced by the external noise. When noise is higher than the threshold value $\xi = 1.5 \times 10^{-5}$ (case c), the velocity of the particle is really affected by the external Gaussian noise.

Thus according to Eq. (8), the particle escapes from the scattering region when the value of the integral $\int_0^{t_e} \dot{x}\xi_x(t) + \dot{y}\xi_y(t)\, dt$ gets the particular value yielded by the normal distribution $T_e - T_0$ at the time escape t_e. When the noise intensity is very weak (for $E_0 = 0.19$, below 1.5×10^{-5}), the influence of the noise over the variation of the velocity is lower than the noise intensity itself [Fig. 11 (a)–(b)]. Therefore the value of the integral $\int_0^{t_e} \dot{x}\xi_x(t)\, dt$ merely depends on the noise $\xi_x(t)$. If we shoot multiple particles with the same initial conditions but different noise intensities, the variance of the different values of the integrals $\int_0^{t_e} \dot{x}\xi_x(t)\, dt$ and the noise intensity shall increase proportionally [Fig. 12 (a)–(b)]. The higher the noise intensity, the more probable is to get a higher value of $|T_e - T_0|$ and, therefore, the higher the integration time, t_e, shall be needed by the integral to get the specific value of $T_e - T_0$. For that reason, the average escape time of a set of particles in the scattering region, $\overline{t_e}$, increases insofar the external weak noise also increases until getting the maximum value shown in Fig. 4. However, when noise is higher than the threshold value $\xi = 1.5 \times 10^{-5}$, the velocity of the particle is really affected by the external Gaussian noise [Fig. 11(c)] and the value of the integral $\int_0^{t_e} \dot{x}\xi_x(t)\, dt$ depends on two factors: the variance of $\dot{x}$ and the variance of $\xi_x(t)$. Then, if we shoot multiple particles with the same initial conditions but different noise intensities, the variance of the different values of the integrals $\int_0^{t_e} \dot{x}\xi_x(t)\, dt$ shall increase much higher than the variance of the noise intensity [Fig. 12(c)]. Therefore the higher the noise intensity $\xi(t)$, the lower the integration time, t_e is requested by
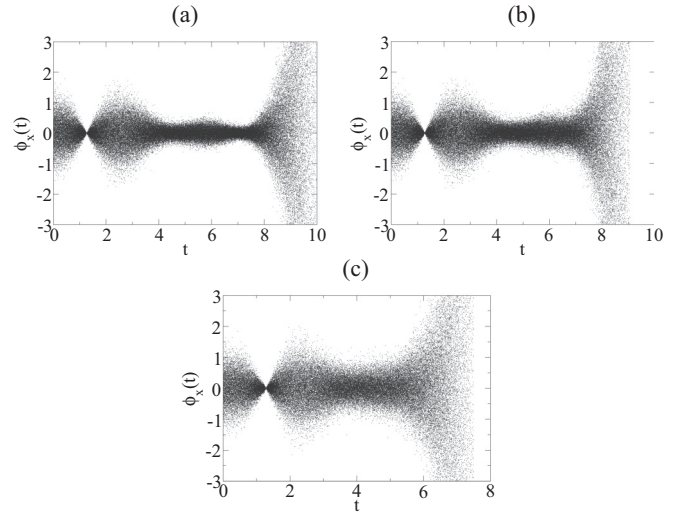

FIG. 12. This set of figures represents the function $\phi_x(t) = \dot{x}\xi_x(t)$ vs time t of a particle shot from (x, y) with initial energy $E_0 = 0.19$ and initial angle $\varphi = \pi/5$. (a) $\xi = 1 \times 10^{-10}$; (b) $\xi = 1.5 \times 10^{-5}$; (c) $\xi = 5 \times 10^{-4}$. For low noise intensities, (cases a–b), the particle velocity is not very influenced by the external noise and then the value of the integral $\phi_x(t)$ merely depends on the noise $\xi_x(t)$. Therefore, if we shoot multiple particles with the same initial conditions but different noise intensities, the variance of the values of the integrals $\int_0^{t_e} \dot{x}\xi_x(t)\, dt$ and the noise intensity shall increase proportionally. However, when noise is higher than the threshold value $\xi = 1.5 \times 10^{-5}$ (case c), the velocity of the particle is really affected by the external Gaussian noise and the value of the integral $\int_0^{t_e} \dot{x}\xi_x(t)\, dt$ depends on two factors, the variance of $\dot{x}$ and the variance of $\xi_x(t)$.

the integral to get the specific value of $T_e - T_0$. For that reason, the average escape time of a set of particles in the scattering region, $\overline{t_e}$, quickly decreases insofar the external weak noise also increases after reaching the maximum shown in Fig. 4.

VI. CONCLUSIONS AND DISCUSSION

There have been relevant steps to understand the effects of an external source of weak Gaussian noise on the behavior of the Hénon-Heiles system in the last few years. Indeed, the presence of noise is characteristic in several physical situations such as in the transport and trapping of chemically or biologically active particles in large-scale flows (see Ref. [28]). The main goal of the present work has been to demonstrate that a source of additive uncorrelated Gaussian noise with an even lower intensity than the former framework studied up to now [14–16] may provide a constructive effect on the system.

We have concluded that when the noise intensity is very weak, from $\xi = 0$ to $\xi = 1.5 \times 10^{-5}$, the average escape time $\overline{t_e}$ increases as the noise increases. Within this noise range, each basin boundary is fractal and not blurred as shown in Fig. 7. For noise intensity values above $\xi = 1.5 \times 10^{-5}$, the fractal structure completely disappears and becomes shaded off. However, when the noise intensity increases from 1×10^{-10} to 1×10^{-7} the morphology of the KAM sets is destroyed and the number of particles which remains in the scattering region

after $t_{\max}$ decreases. Somewhere between $\xi \sim 1 \times 10^{-7}$ and 1×10^{-6}, the number of trapped particles starts to rise and to be spread along the whole phase space. Then, during a certain range of noises, the stickiness formerly given by the KAM sets now loses intensity but gains extension. It has been also corroborated in Figs. 6 and 9. We have also found that the decay law for the Hénon-Heiles system is algebraic when the noise intensity is lower than the threshold value $\xi = 1.5 \times 10^{-5}$. Once the noise intensity exceeds this limit, we have to resort to an exponential decay.

Last, we conjecture that any solution of the noisy Hénon-Heiles system jumps throughout different trajectories from the noiseless system such that all its points correspond to points from noiseless systems in a one-to-one correspondence. From this framework, we can qualitatively explain a very rich variety of phenomena that takes place in the Hénon-Heiles systems in the presence of weak noise. Moreover, considering that the external Gaussian noise affects only the kinetic energy, we suggest a theoretical reasoning to explain why a very low noise intensity stabilizes the system, which seems to be a new constructive effect of noise.

[1] J. M. Seoane and M. A. F. Sanjuán, Rep. Prog. Phys **76**, 016001 (2012).

[2] E. Ott and T. Tél, Chaos **3**, 417 (1993).

[3] M. Hénon and C. Heiles, Astron. J. **69**, 73 (1964).

[4] C. Jung, J. Phys. A **19**, 1345 (1986); M. Hénon, Physica D **33**, 132 (1988); G. Troll and U. Smilansky, *ibid.* **35**, 34 (1989).

[5] S. Bleher, C. Grebogi, and E. Ott, Physica D **46**, 87 (1990).

[6] M. Ding, C. Grebogi, E. Ott, and J. A. Yorke, Phys. Rev. A **42**, 7025 (1990).

[7] C. Grebogi, E. Ott, and J. A. Yorke, Physica D **7**, 181 (1983).

[8] T. Tél, in *Directions in Chaos*, Vol. 3, edited by B. L. Hao (World Scientific, Singapore, 1990), p. 149; in *STATPHYS 19*, edited by B. L. Hao (World Scientific, Singapore, 1996), p. 243.

[9] A. E. Motter and Y.-C. Lai, Phys. Rev. E **65**, 015205(R) (2001).

[10] J. M. Seoane, J. Aguirre, M. A. F. Sanjuán, and Y.-C. Lai, Chaos **16**, 023101 (2006).

[11] J. M. Seoane, M. A. F. Sanjuán, and Y.-C. Lai, Phys. Rev. E **76**, 016208 (2007).

[12] J. Lehmann, P. Reimann, and P. Hänggi, Phys. Rev. Lett. **84**, 1639 (2000).

[13] P. Mills, Commun. Nonlinear Sci. Numer. Simul. **11**, 899 (2006).

[14] J. M. Seoane and M. A. F. Sanjuán, Phys. Lett. A **372**, 110 (2008).

[15] J. M. Seoane, L. Huang, M. A. F. Sanjuán, and Y.-C. Lai, Phys. Rev. E **79**, 047202 (2009).

[16] J. M. Seoane and M. A. F. Sanjuán, Int. J. Bifurcation Chaos **20**, 2783 (2010).

[17] E. G. Altmann and A. Endler, Phys. Rev. Lett. **105**, 244102 (2010).

[18] P. E. Kloeden, E. Platen, and H. Schurz, *Numerical Solution of Stochastic Differential Equations* (Springer, Berlin, 1994).

[19] R. Barrio, F. Blesa, and S. Serrano, Europhys. Lett. **82**, 10003 (2008).

[20] C. F. F. Karney, Physica D **8**, 360 (1983); B. V. Chirikov and D. L. Shepelyansky, *ibid.* **13**, 395 (1984); J. Meiss and E. Ott, *ibid.* **20**, 387 (1986); Y.-C. Lai, M. Ding, C. Grebogi, and R. Blümel, Phys. Rev. A **46**, 4661 (1992).

[21] J. Casado-Pascual, C. Denk, and J. Gómez-Ordóñez, Phys. Rev. E **67**, 036109 (2003).

[22] G. Contopoulos, Astron. Astrophys. **231**, 41 (1990).

[23] E. G. Altmann, A. E. Motter, and H. Kantz, Phys. Rev. E **73**, 026207 (2006).

[24] J. Aguirre and J. C. Vallejo and M. A. F. Sanjuán, Phys. Rev. E **64**, 066208 (2001).

[25] J. Aguirre, R. L. Viana, and M. A. F. Sanjuán, Rev. Mod. Phys. **81**, 333 (2009).

[26] M. A. F. Sanjuán, J. Kennedy, E. Ott, and J. A. Yorke, Phys. Rev. Lett. **78**, 1892 (1997).

[27] M. A. F. Sanjuán, J. Kennedy, C. Grebogi, and J. A. Yorke, Chaos **7**, 125 (1997).

[28] A. E. Motter, Y.-C. Lai, and C. Grebogi, Phys. Rev. E **68**, 056307 (2003).

[29] C. W. Gardiner, *Stochastic Methods: A Handbook for the Natural and Social Sciences* (Springer Complexity, Berlin, 2004).